ELSEVIER

PII: S0032-3861(97)10358-5

Polymer Vol. 39 No. 16, pp. 3675–3681, 1998

0032-3861/98/$19.00+0.00

Toughening of polypropylene by different elastomeric systems

Y. Yokoyama† and T. Ricco*
University of Trento, Department of Materials Engineering, Via Mesiano 77, I38050 Trento, Italy
(Received 1 May 1996; revised 17 September 1997)

Rubber toughening of a series of blends constituted by a polypropylene (PP) matrix added with talc, and modified by ethylene–propylene (EPR) and/or ethylene–butene rubber (EBR), with different molecular weights, was investigated. The fracture toughness was measured by an elasto-plastic fracture mechanics approach, applying the methodology of the essential work of fracture, and by conventional testing. It was found that: (i) EBR has a higher toughening efficiency than EPR; and (ii) the fracture toughness increases by increasing the molecular weight of the dispersed elastomeric phase. Measurements of volume change and temperature increase in specimens stretched during tensile tests indicated that the presence of EBR in the blends reduces cavitation and crazing, and induces a large amount of shear yielding. Some difference in the microcavitation mechanisms induced by each of the two elastomers was shown by electron microscopy analysis. An explanation of this behaviour on the basis of structural changes within the matrix or at the rubber–matrix interface was sought. Dynamic thermomechanical analysis indicated that EBR has a stronger interaction than EPR with the PP matrix.

(Keywords: rubber-modified polypropylene; fracture toughness; essential work of fracture)

INTRODUCTION

The fracture toughness of polypropylene (PP) can be enhanced by rubber modification[1–3]. The incorporation of a secondary rubbery phase in PP is usually achieved both by propylene–ethylene block copolymerization and by mechanical blending of PP with ethylene–propylene rubber (EPR) and ethylene–propylene–diene terpolymer (EPDM)[1–3]. However, it was recently claimed that ethylene–α-olefins have higher toughening efficiency for PP[4–6].

This work aimed at investigating the effect of the incorporation of ethylene–α-olefin rubber within a PP matrix on the mechanical properties and fracture behaviour of these blends. Ethylene–butene rubber (EBR) was selected as the ethylene–α-olefin component, and model compounds consisting of a PP matrix containing talc, EPR and/or EBR at different molecular weights were studied. Post-yielding and fracture behaviour of these materials were investigated. Fracture toughness was evaluated following different methodologies, such as the essential work of fracture method and Izod impact testing. The toughening mechanisms were also investigated.

EXPERIMENTAL

Materials

The materials used in the blends were: high isotactic PP (mm = 99.2%) with MFR = 80, provided by Montell Polyolefins (Ferrara, Italy); EPR and EBR at three different molecular weights, obtained by conventional catalyst technology, and commercially produced by Mitsui Petrochemical Co. Ltd., Japan; and fine particles of talc Micron White 5000P, with average diameter of about 2.9 μm, produced by Hayashi Kasei Co. Ltd., Japan. Some main characteristics of the elastomers employed are shown in *Table 1*. Each level of molecular weight (low, high and intermediate) is comparable between the two elastomers, and it is labelled by the letters L, H and M for EBR and *L*, *H* and *M* for EPR.

The blends, supplied by Montell Polyolefins (Ferrara, Italy), were obtained under the same conditions by a Banbury mixer following the formulations listed in *Table 2*, i.d. maintaining the contents of talc and the total elastomeric component at constant levels, such as 10 and 31.5 wt%, respectively.

The blends were injection moulded in the form of ASTM dumbbell specimens, 127 mm × 12.7 mm × 3.2 mm bars and 127 mm × 127 mm × 2.5 mm plates, under the following moulding conditions: injection temperature 210°C, mould temperature 60°C, injection time 15 s and cooling time 44 s.

Some basic characterization of the materials is reported in *Table 2*.

Microstructural characterization

The morphology of the materials was observed by scanning electron microscopy (SEM) and by optical microscopy.

SEM analysis was carried out on cryogenic fracture surfaces, obtained at high speed from undeformed dumbbell specimens, perpendicular to the melt flow direction. For this purpose, the central portions of specimens were previously notched, immersed in liquid nitrogen and fractured using a Charpy pendulum. In addition, cryogenically microtomed surfaces, cut parallel to the melt flow direction and etched in n-hexane, were observed by SEM.

Measurements by differential scanning calorimetry (d.s.c.) were also performed.

* To whom correspondence should be addressed
† On leave from Showa Denko K. K., 2 Oaza Nakanosu, Oita 870-01, Japan

Table 1 Characteristics of the elastomers

Elastomer	M_n	M_w	M_w/M_n	Comonomer		T_m^a	T_g^b	χ_c^c	MFR[d]	S.G.[e]	E^f
	$\times 10^3$	$\times 10^3$		Species	Wt%	(°C)	(°C)		(%)	(dg min^{-1})	(MPa)
EPR-*L*	46	101	2.2	C3[g]	25	47	− 42	15	8.1	0.870	14
EPR-*M*	70	164	2.3	C3	26	47	− 36	16	1.8	0.871	17
EPR-*H*	90	200	2.2	C3		49	− 35	14	0.8	0.868	13
EBR-L	54	120	2.2	C4[h]	20	53/76	− 35	21	6.7	0.883	35
EBR-M	60	147	2.5	C4	19	51/74	− 34	25	2.5	0.883	36
EBR-H	104	235	2.3	C4		55/74	− 34	20	0.5	0.881	33

[a]Melting temperature. For EBRs two peaks were observed as melting points
[b]Glass transition temperature
[c]Crystallinity
[d]Melt flow rate (230°C, 2.16 kg)
[e]Specific gravity
[f]Tensile elastic modulus
[g]Propylene
[h]Butene

Table 2 Formulation and characterization of the blends

Code	PP (wt%)	EPR-*L* (wt%)	EPR-*M* (wt%)	EPR-*H* (wt%)	EBR-L (wt%)	EBR-M (wt%)	EBR-H (wt%)	Talc (wt%)	Additives (wt%)	MFR[a] (dg min^{-1})	HDT[b] (°C)	R.H.[c]	F.M.[d] (GPa)
1	58.25			15.75			15.75	10.00	0.25	18.6	106	78	1.50
2	58.25			15.75		15.75		10.00	0.25	20.8	109	74	1.48
3	58.25			15.75	15.75			10.00	0.25	23.9	105	81	1.49
4	58.25		15.75			15.75		10.00	0.25	23.1	108	82	1.55
5	58.25		15.75		15.75			10.00	0.25	27.2	109	77	1.58
6	58.25	15.75				15.75		10.00	0.25	28.1	102	82	1.58
7	58.25				31.50			10.00	0.25	31.4	101	83	1.60
8	58.25					31.50		10.00	0.25	23.9	100	84	1.58
9	58.25						31.50	10.00	0.25	18.8	106	84	1.56
10	58.25	31.50						10.00	0.25	33.2	114	75	1.56
11	58.25		31.50					10.00	0.25	23.6	100	76	1.52
12	58.25			31.50				10.00	0.25	17.2	107	76	1.53

[a]Melt flow rate (230°C, 2.16 kg)
[b]Heat distortion temperature
[c]Rockwell hardness
[d]Flexural elastic modulus

Mechanical characterization

Tensile properties were measured at room temperature at a range of cross-head speeds between 2 and 10^3 mm min^{-1} using an Instron testing machine with ASTM dumb-bell specimens.

Fracture mechanics tests at low rate were performed by applying the method of the plane-stress essential work of fracture (EWF)[7,8], following a multispecimen technique. For each blend, a series of sharply notched DEN(T) specimens, obtained from the moulded plates as shown in *Figure 1*, with length $L = 125$ mm, width $W = 50$ mm and thickness $B = 2.5$ mm, and with different ligament lengths, were tested. The particular specimen orientation with respect to the injection gate, chosen as in *Figure 1*, prevented asymmetrical growth of the two cracks due to material orientations within the plates[9]. Four different levels of ligament length were considered ($l = 8$, 10, 13 and 16 mm), so as to match the requirements $3B\langle l\langle W/3$ to avoid the edge effects and to secure the plane-stress condition[8]. For each level of the ligament length, at least four specimens were tested. The tests were carried out using the Instron machine at room temperature and at a cross-head speed of 50 mm min^{-1}.

Conventional Izod impact tests were also carried out. The orientation of the Izod bars to the melt flow direction was as in *Figure 1*.

Heat generation within samples 1, 9 and 12 during tensile tests, carried out using an Instron machine at room temperature and at a cross-head speed of 15 mm min^{-1}, was measured in air using an infrared camera produced by Nippon Avionics Co. Ltd. and recorded by a video recorder.

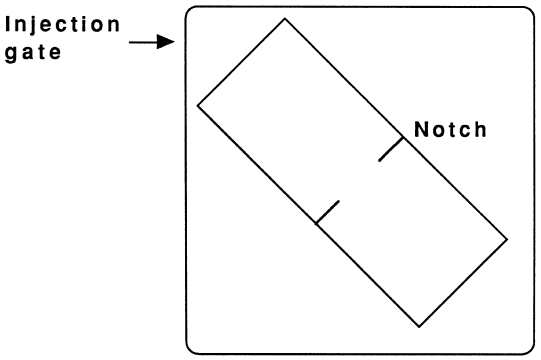

Figure 1 DEN(T) specimen for EWF testing cut from injection-moulded plates. The orientation of the specimens with respect to the position of the injection gate is shown

Measurements of volume change within samples 1, 9 and 12, stretched at different levels of elongation (5, 10, 15, 20, 25, 50, 75 and 100%) by tensile tests carried out under the same conditions, were performed. After reaching each deformation level, the specimens were unloaded and kept at room temperature for 2 days. The specific gravity of samples, cut from the deformed specimens in the region where necking took place, was measured at 21°C in ethyl alcohol at 99.5% of purity following the ASTM D-792 standard. The specific gravity of ethyl alcohol was

interpolated at the actual testing temperature using the Smithsonian Tables[10]. The volume change within the deformed specimens, normalized with respect to the initial volume, $\Delta V/V$, was determined according to the relationship $\Delta V/V = \rho/\rho^* - 1$, ρ and ρ^* being the specific gravity before and after deformation, respectively.

For each of the blends 1, 9 and 12, SEM and transmission electron microscopy (TEM) analysis were performed on samples taken from dumb-bell specimens previously deformed in tension up to 15% under the conditions indicated above. SEM observations were carried out from the EDGE view on microtomed surfaces sputtered by gold. TEM observations were performed from the EDGE view on ultra-thin microtomed sections stained by RuO_4.

Dynamic thermomechanical analysis (DMTA) was also performed on samples 1, 9 and 12 using a Polymer Laboratory instrument in the temperature range from −100°C up to 100°C, at a frequency of 10 Hz in bending mode.

RESULTS AND DISCUSSION

Phase morphology

Optical microscopy analysis performed on the moulded samples showed a typical skin–core structure, though the skin–core boundary was not so clear and sharp as is usually observed for PP/EPR samples[11]. Furthermore, no spherulitic structure was observed.

D.s.c. measurements indicated that in all the materials the degree of crystallinity of the PP matrix remained constant (about 69% within the core of the specimens and 65% within a 0.7-mm-thick superficial layer).

SEM micrographs of cryogenic fracture surfaces obtained perpendicular to the melt flow direction showed that the elastomeric particles were finely dispersed in the PP matrix and their sections had a more or less circular shape. Typically, the particle sizes decreased by decreasing the molecular weight of the elastomer, in agreement with the results of D'Orazio *et al.*[12]. Comparing the blends containing only EBR with those containing only EPR, the dispersion of the rubber particles appeared very similar at each level of rubber molecular weight.

SEM micrographs of the etched fracture surfaces parallel to the melt flow direction revealed that the shape of the particles was strongly elongated along the melt flow direction, due to the injection moulding process[13].

Post-yielding and fracture behaviour

In order to clarify the effect of the hybridization of the elastomeric phase, the yield and post-yield behaviour of the blends were analysed as a function of the EBR content in the total elastomeric component.

All the materials exhibited stress whitening before the yield point, and the blends containing only EPR (samples 10–12) showed a necking less pronounced than the others. For the three blends 9, 12 and 1, typical load–displacement curves obtained in tensile tests are shown in *Figure 2*. Typically, the materials showed a yield point at elongation of about 7–8%, at which the necking process took place and then continued up to an elongation of about 50–70%. After necking, the cold-drawing process for samples 9 and 1 was initiated, whereas for sample 12 breakage occurred. For each material, stress whitening of the specimens was observed to initiate close to the yielding point.

The yield strength and the elongation at break, evaluated at a cross-head rate of 15 mm min^{-1}, are plotted in *Figures 3* and *4*, respectively. Considering that the molecular weights of the two rubbers are very close for each of the three different levels of molecular weight considered [high (*H*, H), low (*L*, L) and intermediate (*M*, M)], curves

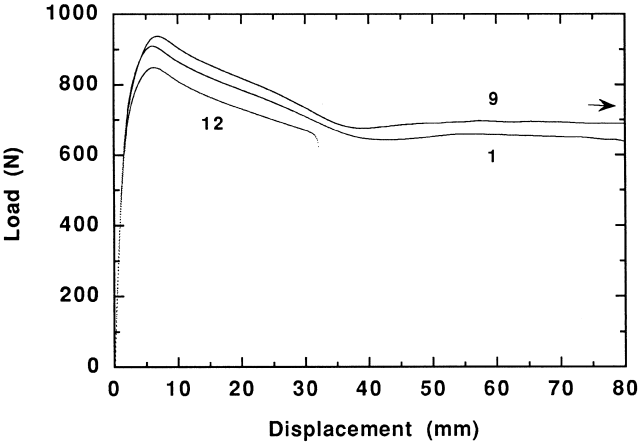

Figure 2 Typical load–displacement curves obtained in tensile tests at room temperature and at a cross-head rate of 15 mm min^{-1} for PP/EBR/talc (sample 9), PP/EPR/EBR/talc (sample 1) and PP/EPR/talc (sample 12)

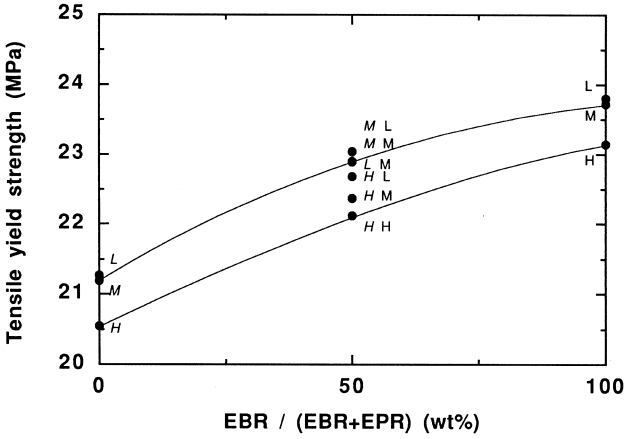

Figure 3 Tensile yield strength of the blends *versus* the EBR content in the total elastomeric component. The letters *H*, *L*, *M* and H, L, M indicate the high, low and intermediate molecular weights of EPR and EBR, respectively

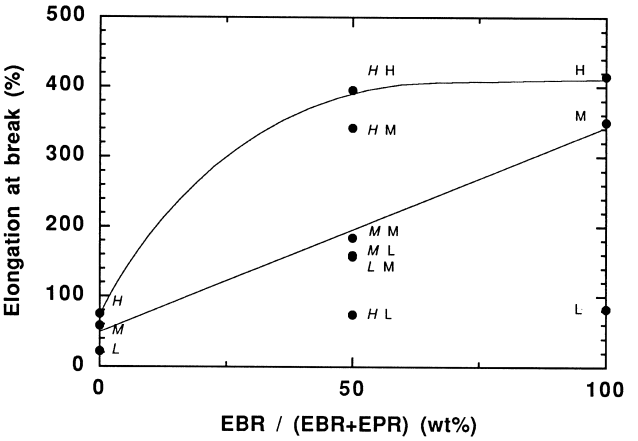

Figure 4 Elongation at break of the blends, measured in tensile tests at a cross-head rate of 15 mm min^{-1}, *versus* the EBR content in the total elastomeric component. The letters in the figure have the same meaning as in *Figure 3*

connecting points relative to the same level of rubber molecular weight were drawn in *Figures 3* and *4*, as well as in the following. Typically, it was found that PP/EBR/talc blends show both higher yield strength and elongation at break than PP/EPR/talc blends. By increasing the molecular weight of the elastomers, however, the yield strength decreases and the elongation at break increases. The latter effect is particularly marked for the blends containing only EBR in the elastomeric phase. Furthermore, for the rubbers at high molecular weight (*H* and H), the elongation at break of the blends shows a pronounced upper deviation from the linear additivity rule as a function of the EBR content in the elastomeric component, whereas for the rubbers at intermediate molecular weight (*M* and M) the linear additivity rule is obeyed. This indicates that the addition of high-molecular-weight EBR strongly enhances the cold-drawing process after yielding. For the compounds containing the elastomers at high molecular weight (samples 1, 9 and 12), the elongation at break is also shown as a function of the testing rate in *Figure 5*. The samples containing EBR (1 and 9) undergo quite a sharp transition from a high to a low level of the ultimate elongation at rates between 10 and 50 mm min^{-1}.

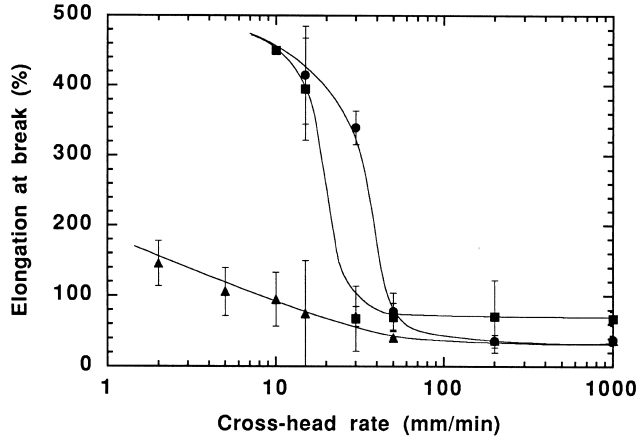

Figure 5 Elongation at break versus cross-head rate in tensile tests for samples 1 (■), 9 (●) and 12 (▲)

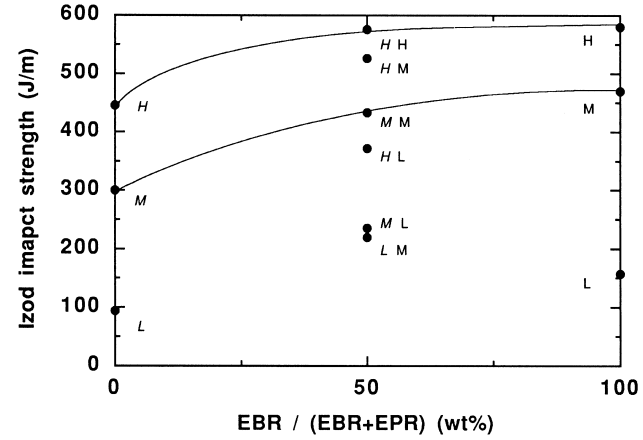

Figure 6 Izod impact strength of the blends *versus* the EBR content in the total elastomeric component. The letters in the figures have the same meaning as in *Figures 3* and *4*

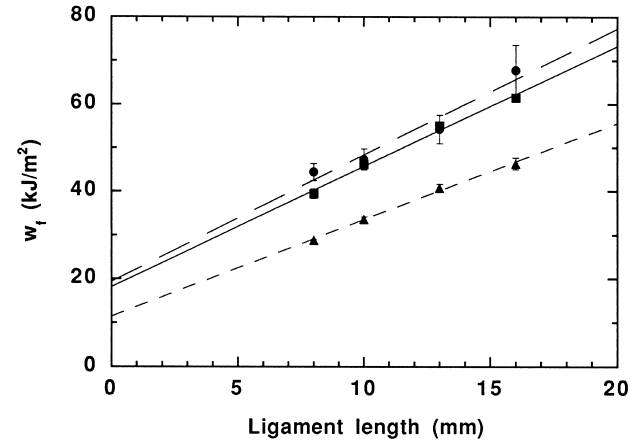

Figure 7 Specific total work of fracture *versus* ligament length measured by DEN(T) specimens for samples 1 (■), 9 (●) and 12 (▲) in EWF testing

The fracture behaviour of the materials was firstly characterized by conventional testing. Notched Izod impact strength, reported in *Figure 6* as a function of the EBR content in the elastomeric portion, was found to increase by increasing the molecular weight of the rubbers, in agreement with the results of other authors[3,5,14,15]. Furthermore, EBR appears to be generally more efficient than EPR in promoting toughening in PP. Similarly, Cieslinski *et al.*[5] found that ethylene–octene copolymer is better than EPDM rubber to toughen PP. An upper deviation from the linear additivity rule is also shown by the Izod impact strength, particularly marked for the rubbers with high molecular weight.

In EWF testing, to evaluate the essential work of fracture, w_e, the total energy to fracture, w_f, normalized with respect to the resistant section of the specimens, was plotted *versus* the specimen ligament length, l, as shown in *Figure 7* for samples 1, 9 and 12. The experimental data were linearly interpolated according to the relationship $w_f = w_e + \beta w_p l$[7,8], where w_e is the essential work of fracture (per fracture surface unit) and represents the energy dissipated in the fracture process zone, whereas βw_p is the density of the energy dissipated in the outer plastic zone, whose shape is taken into account by the dimensionless factor β. It has been proposed that w_e is a true material property which characterizes the material fracture resistance under plane-stress conditions[7,8]. The values of w_e were determined for each material from the straight line w_f *versus* l, such as those of *Figure 7*, by extrapolation to zero ligament length. The low-rate values of w_e are reported in *Figure 8a* as a function of the EBR content in the elastomeric mixture. *Figure 8b* shows the effect of rubber molecular weight on w_e for the blends containing a single elastomeric component (EBR or EPR). The behaviour of w_e qualitatively confirms the results obtained in the impact fracture experiments, though the different methods adopted appear to have a different sensitivity both to the type of the elastomeric component and to the molecular weight of the elastomers present in the blends. However, due to the meaning of the intrinsic material property attached to w_e, the amount of w_e increase, with increasing both the EBR content in the rubbery component and the rubber molecular weight, definitely proves and intrinsically quantifies the enhancement of the low-rate fracture toughness. For elasto-plastic behaviours and in plane-stress conditions, the increment of fracture toughness associated with the increase of the EBR content in the elastomeric phase is higher than that obtained by increasing the rubber molecular weight, at least in the ranges of molecular weight considered.

Figure 9 shows that the w_e data do not have a clear

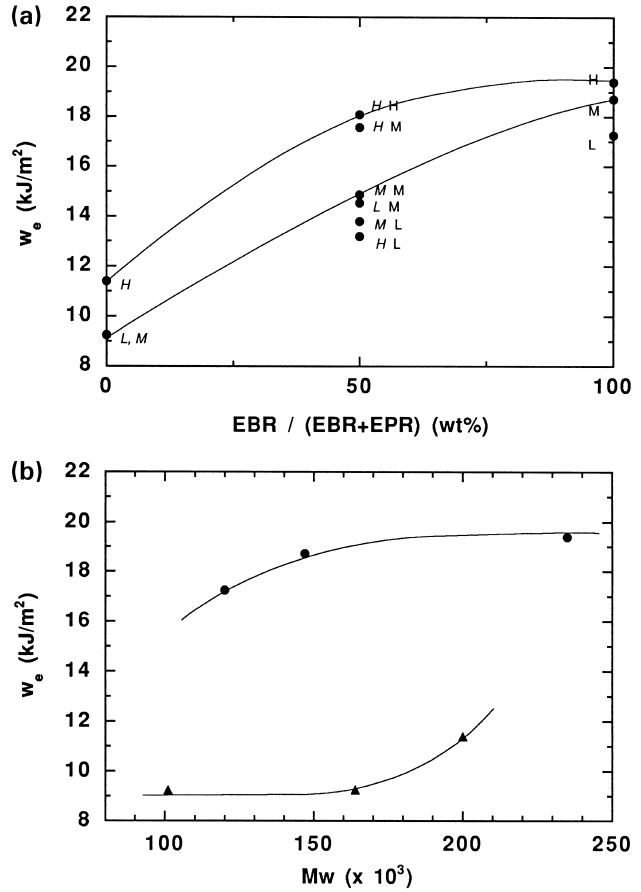

Figure 8 (a) Essential work of fracture of the blends *versus* the EBR content in the total elastomeric component (the letters in the figure have the same meaning as in *Figures 3, 4, and 6*). (b) Essential work of fracture *versus* rubber molecular weight for the blends containing a single elastomeric component: (●) EBR; (▲) EPR

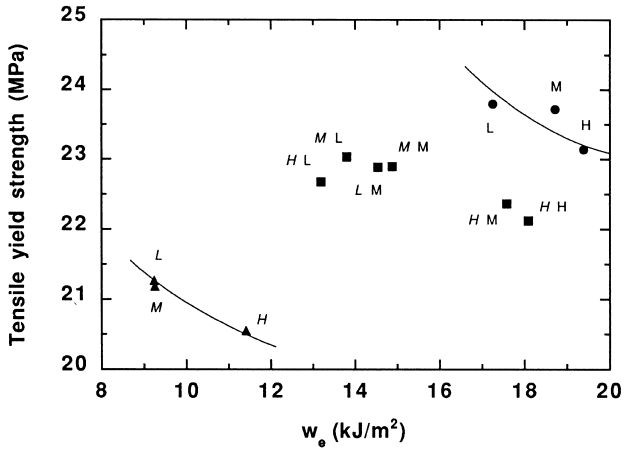

Figure 9 Tensile yield strength against the essential work of fracture for the materials investigated

correlation with those of the yield strength. In particular, the decrease of the yield strength does not necessarily imply an increase of w_e, notwithstanding that it is generally thought that a decrease of the yield strength corresponds to an enhancement of fracture toughness, so that in rubber-modified crystalline polymers the achievement of a reduction of the yield strength is considered as an index of toughening[16,17]. However, this expected correlation is found within each of the two categories of blends containing only EPR or EBR, respectively.

Since the increase of the rubber molecular weight produces an increase of the size of the elastomeric domains, which implies an increase of the interparticle distance, the results obtained seem to contradict the interparticle distance model[18,19]. On the other hand, this model, which takes into account only changes of rubber morphology, is known to govern toughening of rubber-modified PP[10,20–23], as well as of other rubber-modified polymers[18,19], though its applicability cannot be explained only on a mechanical basis[16]. Therefore, the results obtained indicate that the effect of the characteristics of the elastomeric component, such as the chemical nature of rubber and its molecular weight, surpasses the effect of rubber morphology on the development of fracture toughness. This could be ascribed to some changes induced in the matrix, presumably at the rubber/matrix interface, by the different types of rubber.

Toughening mechanisms

Data of volume change in tensile tests are shown in *Figure 10* as a function of percentage elongation for blends 9, 12 and 1. For sample 12, it was not possible to collect data for elongation higher than 70% due to the breakage of the specimen. For the three materials, different extents of volume increase with increasing specimen elongation are observed. Sample 12 exhibits the highest volume increase, which is maintained at about twice that of sample 9 over the whole range of elongation explored, whereas sample 1 shows an intermediate behaviour. These results indicate that the presence of EPR in the blend favours dilatation processes, which could be envisaged as crazing, voiding and/or cavitation. In fact, a higher cavitation resistance induced by EBR should be expected because of its higher elastic modulus[17]. Furthermore, *Figure 10* shows that the cavitation mechanisms start before the yield point at low strains, as also occurs in rubber-toughened polyamide[17,21].

The temperature profile within the specimens during the tensile tests indicated that, in the necking region, the temperature is higher than in the surrounding regions[22]. For each material, the temperature increase within the necking region is shown in *Figure 11* as a function of elongation. After the yield point the blends containing EBR, i.e. samples 9 and 1, showed a more pronounced temperature increase. It is well known that, when plastic deformation takes place, heat can be generated within the specimen by shear, entropy

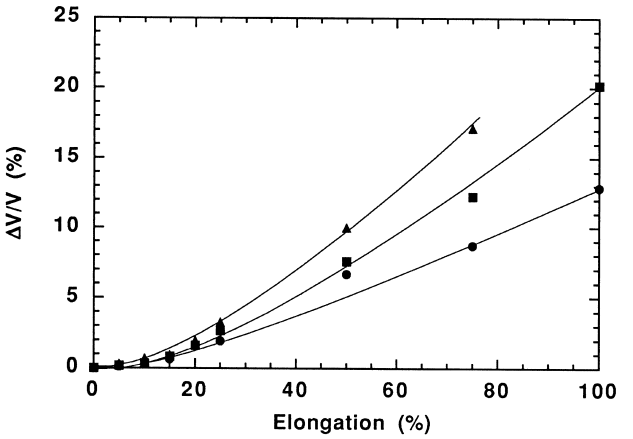

Figure 10 Volume increase inside the neck region of dumb-bell specimens *versus* percentage elongation in uniaxial tensile tests performed at room temperature and at a cross-head speed of 15 mm min^{-1}. (●) Sample 9 (PP/EBR/talc); (■) sample 1 (PP/EPR/EBR/talc); (▲) sample 12 (PP/EPR/talc)

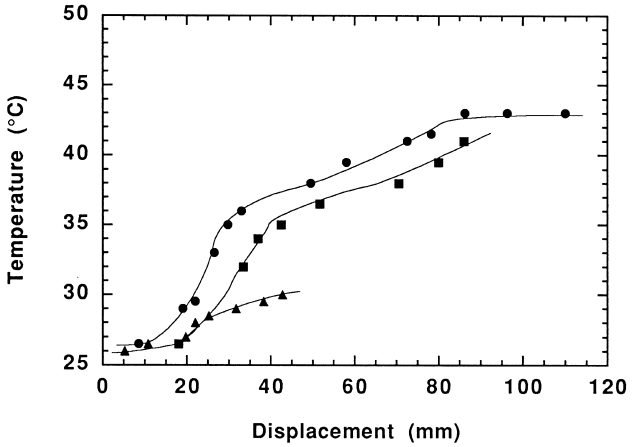

Figure 11 Temperature increase inside the neck region of tensile specimens, in uniaxial tensile tests performed at room temperature and at a cross-head speed of 15 mm min^{-1}, as a function of displacement. (●) PP/EBR/talc (sample 9); (■) PP/EPR/EBR/talc (sample 1); (▲) PP/EPR/talc (sample 12)

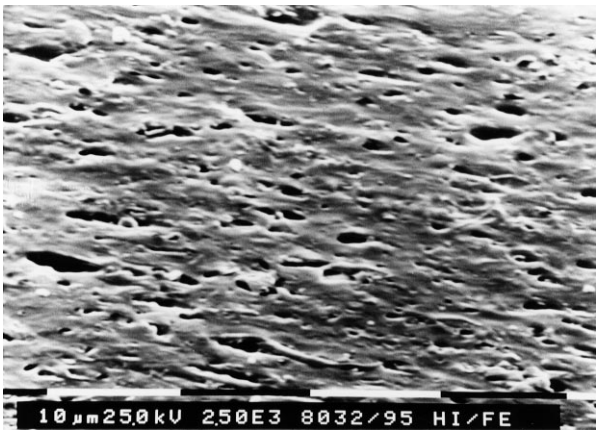

Figure 12 SEM micrographs from the EDGE view of PP/EBR/talc (sample 9) after uniaxial tension up to 15% elongation, taken inside the neck region. The direction of the applied load is parallel to the drawn axis. Scale bar = 10 μm

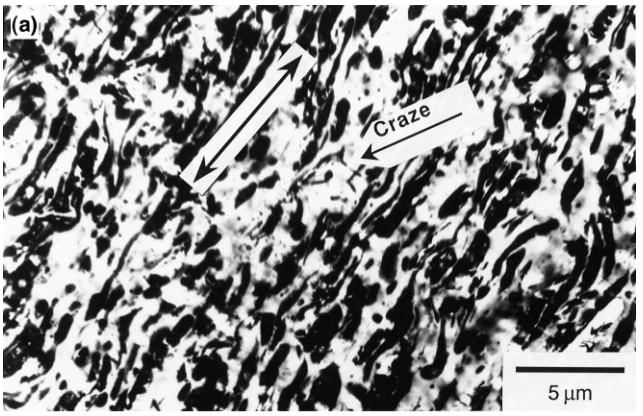

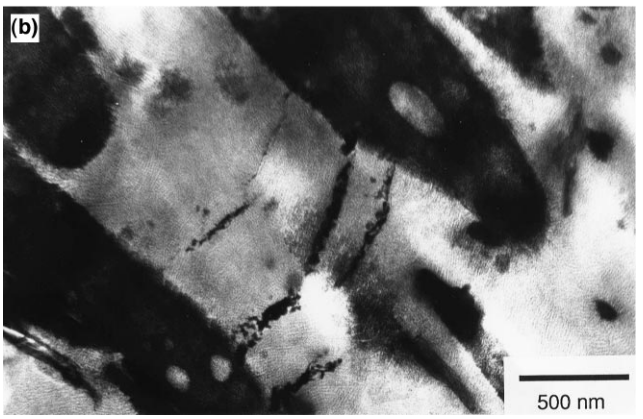

Figure 13 (a) TEM micrographs of the EDGE view of PP/EBR/talc (sample 9) after uniaxial tension up to 15% elongation, taken inside the neck region. The arrow indicates the direction of the applied load. Crazing is also indicated. (b) Higher magnification of zones within the micrograph shown in (a)

loss by molecular orientations and release of internal energy[23]. Assuming that the heat loss, and the consequent temperature increase, is mostly due to shear[24], the results obtained indicate that samples 9 and 1 have a higher disposition to undergo shear yielding.

SEM analysis of the EDGE view of samples 9 and 12, deformed at the elongation of 15%, revealed the presence of voids as shown by the micrograph of *Figure 12*, taken inside a stretched specimen of sample 9. The elongated shape of the elastomeric domains in this figure must be attributed mainly to the injection moulding process, as remarked above. For sample 12, larger and more conspicuous cavities were observed.

Evidence of craze formation was found in both samples 9 and 12 by TEM analysis. *Figure 13a* shows a TEM micrograph of the EDGE view of an ultramicrotomed specimen of sample 9 stretched up to 15% of elongation (it was not possible to obtain specimens for TEM at higher levels of elongation). Rubber particles elongated along the melt flow direction due to the injection moulding are observed, as well as spherical particles, which might be created by the breakage of rubber droplets[25]. Crazes running perpendicular to the longer axis of the elastomeric particles, i.d. normal to the tensile direction indicated by the arrow in *Figure 13a*, are observed. A TEM micrograph of the same sample at higher magnification is shown in *Figure 13b*. In sample 12, crazes appeared to be systematically more developed, thicker and with a finer internal structure than in sample 9. The craze thickness was found to be approximately 40 nm in sample 9 and about 80 nm in sample 12.

On the whole, the results obtained indicate that the addition of EBR induces a more extensive shear yielding in the matrix, whereas the addition of EPR produces a larger total amount of dilatation processes, though the contribution of different cavitation mechanisms was not recognized. This result seems to disagree with the results reported for polyamide toughened with different types of rubber[17], which show that the blends with the best fracture behaviour cavitate more easily, since cavitation is able to cause shear yielding in the matrix by relieving the hydrostatic tension at the notch tip[26]. Therefore, the reason for the higher capability of EBR than EPR to promote shear yielding in the PP matrix, responsible for its higher toughening efficiency, must be sought with respect to a difference induced in the matrix itself, or at the rubber/matrix interface, by the two different rubbers.

However, no difference in the degree of crystallinity and in the crystalline structure was shown by d.s.c. experiments and X-ray analysis, respectively. In particular, the presence of a β-crystalline structure, which is known to promote plastic deformation[27], was not found. Furthermore, the orientation of lamellae in the matrix at the rubber/matrix interface, which was proposed to play an important role in

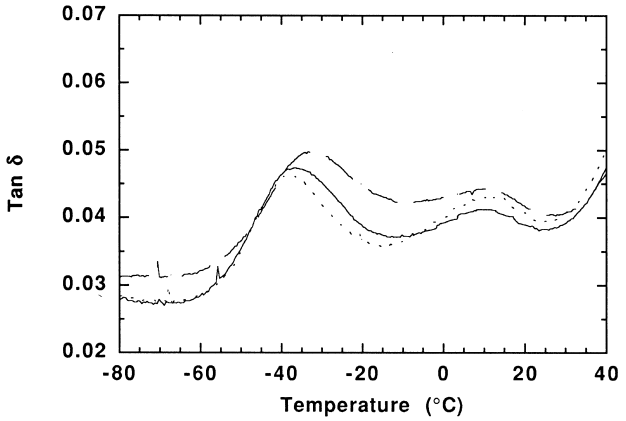

Figure 14 Tan δ as a function of temperature by DMTA for PP/EBR/EPR/talc (full line), PP/EBR/talc (dashed line) and PP/EPR/talc (dotted line)

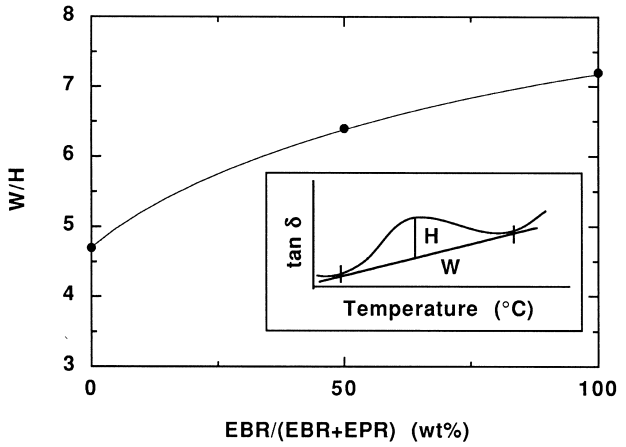

Figure 15 Broadening of the T_g peak of PP for the blends examined, evaluated as indicated in the insert, as a function of the EBR content in the total elastomeric component

the development of fracture toughness of rubber-modified polyamide[16], was not found to be significantly different between the samples containing only EBR or EPR, respectively. In both materials, PP lamellae penetrated into the dispersed elastomeric particles and, typically, were normal to the rubber/matrix interface, as shown in *Figure 13b* for sample 9. No significant difference in the orientation and dimension of the lamellae could be found.

Figure 14 shows tan δ *versus* temperature data obtained by DMTA performed on the samples studied. For each material, the peak at lower temperature concerns the glass transition temperature of the elastomeric phase, whereas the peak at higher temperature is that of PP. Interaction between rubber and matrix can provide shift and broadening of this peak. It is possible to observe in *Figure 14* that the shape of the T_g peak of PP changes appreciably by changing the type of rubber contained in the blend, whereas no significant shift of this peak is found. The broadening of the T_g peak of PP was quantified by introducing the ratio W/H, between the peak width and height, evaluated as shown in the insert of *Figure 15*. Assuming that an increase of W/H is representative of an increased rubber/matrix interaction, the result of *Figure 15* shows that EBR has a stronger interaction than EPR with the PP matrix. The understanding of the nature of this interaction requires further investigation.

CONCLUSIONS

Toughening of PP by the addition of an elastomeric component consisting of EPR and/or EBR, with different molecular weights, was studied by the application of the method of the essential work of fracture.

It was found that, for a constant level of the total rubber content, the incorporation of EBR in the elastomeric component strongly enhanced the fracture toughness of PP blends. Improvement of the fracture resistance was also obtained by increasing the molecular weight of the elastomers.

The higher efficiency of EBR with respect to EPR to toughen PP is due to a higher capability to induce extensive shear yielding within the matrix, in spite of a lower tendency to cause cavitation. Such an effect is attributed to a different interaction exhibited by EBR and EPR with the PP matrix.

ACKNOWLEDGEMENTS

The authors wish to thank 'G. Natta' Research Centre of Montell Polyolefins (Ferrara, Italy) for preparing the samples and supplying some routine characterization. In particular, the authors are grateful to Drs E. Marchetti, A. Pelliconi and D. Tartari for helpful discussions.

REFERENCES

1. Karger-Kocsis, J., ed., *Polypropylene: Structures, Blends and Composites, Copolymers and Blends*, Vol. 2. Chapman and Hall, London, 1995.
2. Bucknall, C. B., *Toughened Plastics*. Applied Science, London, 1977.
3. van der Ven, S., *Polypropylene and Other Polyolefins: Polymerization and Characterization*. Elsevier, Amsterdam, 1990.
4. Nomura, T., Nishio, T., Izanami, K., Yokomizo, K., Kitano, K. and Toki, S., *J. Appl. Polym. Sci.*, 1995, **55**, 1307.
5. Cieslinski, R. C., Silvis, H. C. and Murry, D. J., *Polymer*, 1995, **36**, 1827.
6. Yu, T. C. and Wagner, G. J., *Soc. Plastics Eng. RETEC, Polyolefins* **VIII**, 1993, p. 539.
7. Cotterell, B. and Reddell, J. K., *Int. J. Fract.*, 1977, **13**, 267.
8. Mai, Y. W. and Cotterell, B., *Int. J. Fract.*, 1986, **32**, 105.
9. Yokoyama, Y. and Riccò, T., *Plast. Rubber Comp. Proc. Applic.*, 1996, **25**, 417.
10. West, R. C., ed., *Handbook of Chemistry and Physics*, 6th edn. CRC Press, Boca Raton, FL, 1986–1987, p. F-3.
11. Kantz, M. R., Newmann, H. D. Jr. and Stigale, F. H., *J. Appl. Polym. Sci.*, 1972, **16**, 1249.
12. D'Orazio, L., Mancarella, C., Martuscelli, E. and Polato, F., *Polymer*, 1991, **32**, 1186.
13. Karger-Kocsis, J. and Csikai, I., *Polym. Eng. Sci.*, 1987, **27**, 241.
14. Milani, F., Lori, D. and Massari, P., Preprints, *Third European Symposium on Polymer Blends*, Cambridge, UK, 1990, pp. E/18/1–E/18/4.
15. D'Orazio, L., Mancarella, C., Martuscelli, E. and Sticotti, G., *Polymer*, 1993, **34**, 3671.
16. Muratoglu, O. K., Argon, A. S., Cohen, R. E. and Weinberg, M., *Polymer*, 1995, **36**, 921.
17. Borggreve, R. M., Gaymans, R. J. and Eichenwald, H. M., *Polymer*, 1989, **30**, 78.
18. Wu, S., *Polymer*, 1985, **26**, 1855.
19. Wu, S., *J. Appl. Polym. Sci.*, 1988, **35**, 549.
20. Akiyoshi, R., Tagashira, K. and Izumi, Z., *Polymer Preprints, Japan*, 1990, **39**, 2475.
21. Lazzeri, A. and Bucknall, C. B., *J. Mater. Sci.*, 1993, **28**, 6799.
22. Maher, J. W., Haward, R. N. and Hay, J. H., *J. Polym. Sci.*, 1980, **18**, 2169.
23. Yokobori, T. and Narisawa, I., *Koubunshi Zairyou Kyodogaku*. Ohmu, Tokyo, 1982, p. 80.
24. Wu, S., *J. Polym. Sci., Polym. Phys. Ed.*, 1983, **21**, 699.
25. Han, C. D., *Multiphase Flow in Polymer Processing*. Academic Press, New York, 1981.
26. Yee, A. F., Dongming Li and Xiaowei Li, *J. Mater. Sci.*, 1993, **28**, 6392.
27. Aboulfaraj, M., G'Sell, C., Ulrich, B. and Dahoun, A., *Polymer*, 1995, **36**, 731.